Nonlinear normal modes and local bending vibrations of H_3^+ and D_3^+

D. A. Sadovskiĭ[a)]
Herzberg Institute of Astrophysics, National Research Council, Ottawa, Ontario, Canada, K1A 0R5

Nicholas G. Fulton, James R. Henderson, and Jonathan Tennyson
Department of Physics and Astronomy, University College, Gower St., London WC1E 6BT, United Kingdom

B. I. Zhilinskiĭ[b)]
Laboratoire de spectroscopie hertzienne, Université de Lille I, bâtiment P. 5, 59655 Villeneuve d'Ascq Cedex, France

(Received 28 December 1992; accepted 7 April 1993)

The structure of bending overtones of the H_3^+ and D_3^+ molecular ions at the energies below the barrier to linearity is analyzed using energies and wave functions from full three-dimensional discrete variable representation calculations. The lowest-in-energy states of the vibrational polyads $v_2=4,5,6$ are shown to follow the localization pattern of local bending modes, three equivalent-by-symmetry principal periodic trajectories of the corresponding classical two-mode system near the equilibrium.

I. INTRODUCTION

Since the early days of molecular mechanics harmonic (i.e., linear) normal mode classification has dominated the discussion of molecular vibrations near the equilibrium.[1] At certain excitations, the energy of which depends on how nonrigid a particular molecule is, the system becomes strongly nonlinear. In this case one can switch to more general methods of classical mechanics, such as periodic trajectory analysis, to understand the dynamics of the molecular motion. On the other hand, to compute the quantum energy spectrum one must in general resort to (multidimensional) variational calculations. The recent study of the "horseshoe states" of the H_3^+ molecular ion[2] is a good example of such an approach.

Perhaps because of the quantum-classical correspondence principle, nonlinear dynamics analysis is not usually applied to the lower states of molecules, where the simple normal mode approach is generally assumed to be appropriate. However, molecules are inherently nonlinear systems due to strong anharmonicity effects. In many cases, even at energies as low as those of vibrational fundamentals, molecules behave very differently from the plain linearized picture.

If we associate *the modes of a nonlinear dynamical system* with periodic trajectories two different situations may be easily distinguished.

Almost linear problems

Linear, or harmonic, approximation is well defined: Harmonic frequencies are nonzero ($\omega_i>0$), and there are no resonances ($\omega_i\neq\omega_j$ if $i\neq j$). The set of periodic trajectories at low energies (near the equilibrium) correlates with the normal modes of the linearized system. In particular, their numbers are the same.

Essentially nonlinear problems

(a) Linear approximation applies only at very low energies. However, with increasing energy, periodic trajectories rapidly bifurcate (due to strong anharmonic couplings), so that already at the energies of one vibrational quantum the set of (stable and unstable) periodic trajectories, or nonlinear modes, differs qualitatively from the normal mode set, e.g., the number of such trajectories is larger.

(b) Linear approximation is ambiguous: There are some resonances or zero harmonic frequencies, i.e., certain special *a priori* properties of the molecular Hamiltonian, such as finite group symmetry, cannot be properly represented by linearization. In this case the set of periodic trajectories arbitrarily close in energy to the equilibrium differs from any possible normal mode set. It is important to stress that like the normal modes such a set of (principal) periodic trajectories of a resonance symmetric Hamiltonian system near equilibrium is mainly defined by symmetry, i.e., is not dependent on the particular form of the Hamiltonian under study. To reflect the fundamental role such trajectories play in understanding the dynamics of the system they are called *nonlinear normal modes*.[3]

The best known example of kind (a) is the water molecule, where coupling of symmetric (SS), and antisymmetric (AS) stretching modes causes the appearance of a pair of new equivalent-by-symmetry stable periodic trajectories called *local modes*[4] (LM's). Already at the energy of one stretching quantum the classical analog of this system possesses four principal periodic trajectories:[5] AS (stable), SS (unstable), and two LM's.

[a)]Current address: Department of Physics, College of William & Mary, Williamsburg, VA 23185.

[b)]On leave from Department of Chemistry, Moscow State University, Moscow, Russia, 119 899.

 0021-9606/93/99(2)/906/13/$6.00

Probably the simplest example of kind (b) is the doubly degenerate bending vibration of a triatomic D_{3h} symmetric molecule. In this case the corresponding classical system has eight principle periodic trajectories near equilibrium (compared to the two modes of the linearized problem with continuous symmetry). This molecular problem is equivalent to the near-equilibrium analysis of the well-known Hénon–Heiles Hamiltonian,[6] whose eight nonlinear normal modes are called $\Pi_{7,8}$(stable), $\Pi_{1,2,3}$(stable), and $\Pi_{4,5,6}$(unstable).[3,7]

As we show in the present paper three stable nonlinear (bending) normal modes, $\Pi_{1,2,3}$, of a D_{3h} symmetric triatomic molecule are associated with *local bending*; a classical motion characterized by a predominant deformation of one of the three valence angles of the molecule. In the vibrational energy spectrum such localized states form quasidegenerate triads. More evidence of the localization near $\Pi_{1,2,3}$, which correspond to the three C_2 symmetry axes in the configuration space of the molecule, can be obtained from analyzing the wave function. We use the results of Henderson, Tennyson, and Sutcliffe[8] for H_3^+ and new calculations on D_3^+ to demonstrate that such a localization does indeed occur.

II. NONLINEAR NORMAL MODES OF A D_{3h} SYMMETRIC TRIATOMIC MOLECULE

If a classical Hamiltonian function (on a $2n$-dimensional phase space, where n is the number of degrees of freedom) can be approximated near a potential minimum by a nondegenerate harmonic oscillator (the linearized system is nonresonant), the complete nonlinear Hamiltonian system possesses families of periodic oscillations, or *nonlinear normal modes*, which converge towards a normal mode of linearization. In this case the number of nonlinear normal modes is the same as the number of degrees of freedom.

In the case of resonance and especially in the presence of symmetry the situation becomes more complicated. As shown by Montaldi, Roberts, and Stewart,[3,9] many characteristics of the periodic trajectories near equilibrium (nonlinear normal modes) in the case of resonance and in the presence of symmetry can be directly obtained from a group theoretical treatment, in particular by studying the group action on the set of classical trajectories and implementing the Weinstein–Moser theorem. The important point of such an analysis is the possibility of studying periodic trajectories over the whole initial phase space. In this way possible families of periodic solutions near an equilibrium, or nonlinear normal modes, are characterized by their isotropy group which is a subgroup of the symmetry group acting on the set of trajectories.

On the other hand, an n-dimensional oscillator problem near an equilibrium inherits the dynamical symmetry of its linearization and possesses additional approximate integral(s) of the motion.[10] A particular important example is an approximately conserved action

$$J=\sum I_k, \quad k=1,...,n, \tag{1}$$

where I_k is the action variable of kth oscillator. The corresponding quantum case has an SU(n) approximate dynamical symmetry with the total number of quanta

$$2J=N=\sum a_k^\dagger a_k, \quad k=1,...,n, \tag{2}$$

the Casimir operator of SU(n), as a good quantum number. The spectrum of this quantum problem is formed by vibrational polyads, quasidegenerate groups of states with the same total number of quanta, so that N is often called a polyad number. Such a polyad approximation has a wide range of applications in molecules.[11] Thus it applies even for a floppy molecule such as H_3^+ provided one is close enough (in energy) to the equilibrium; a requirement which does not interfere with the nonlinear normal mode analysis.

Taking advantage of the approximate dynamical symmetry, one can transform the initial problem to a simpler one defined over a *reduced phase space*. The stationary points in such a reduced phase space correspond to periodic trajectories in the complete phase space. In our case the dimension of this space is $2(n-1)$ and the topology of it is that of CP_{n-1}.[12,13] Since CP_{n-1} is a compact space, the analysis of the group action on it together with its topological properties gives a complete set of critical orbits,[14] i.e., a set of points necessarily stationary for any symmetric Hamiltonian defined on this space. As demonstrated by Sadovskiĭ and Zhilinskiĭ for a number of problems,[15] the analysis of critical orbits on the reduced phase space is essentially adequate for and gives the same set of nonlinear normal modes as the direct study of the periodic trajectories of the full initial problem near equilibrium. We comment below on the application of this analysis to a D_{3h} symmetric triatomic molecule.

Such a molecule has two normal modes, a totally symmetric "breathing" mode, ν_1, and a doubly degenerated E'-type bending mode, ν_2. We note that the actual symmetry group acting on the vibrational variables q_1, q_{2x}, and q_{2y}, and hence on any quantities constructed from them, is a group smaller than D_{3h} since the σ_h operation of D_{3h} leaves all the coordinates invariant. Thus, the action of the D_{3h} group on the configuration space itself is equivalent to the natural action of the C_{3v} group with the C_3 axis corresponding to q_1. It is said that the *image* of the D_{3h} group in the $A_1' \oplus E'$ representation (spanned by vibrational coordinates) is the C_{3v} group. It is the C_{3v} group which should be considered when studying the action of the molecular symmetry group, D_{3h}, on the periodic trajectories in the total phase space of the problem.[16]

A. Two-mode case: $\nu_2(E')$ mode

If we consider only the bending vibrations near the equilibrium our problem becomes an analog of the Hénon–Heiles Hamiltonian at low energies with the approximate integral of the motion

$$J=2N=\tfrac{1}{2}(a_x^\dagger a_x+a_y^\dagger a_y)=\tfrac{1}{4}(p_x^2+p_y^2+q_x^2+q_y^2). \tag{3}$$

Equation (3) gives the well-known Schwinger representation of the angular momentum[17] with the components as follows:

$$J_+ = (J_-)^\dagger = a_x^\dagger a_y,$$
$$2J_2 = = i(J_+ - J_-) = p_x q_y - p_y q_x,$$
$$2J_1 = (J_+ + J_-) = p_x p_y + q_x q_y, \tag{4}$$
$$2J_3 = a_x^\dagger a_x - a_y^\dagger a_y = \tfrac{1}{2}(p_x^2 - p_y^2 + q_x^2 - q_y^2).$$

The relation of the components (J_1,J_2,J_3) to the actual reference frame of (q_x,q_y) can be derived by studying the transformation properties of $J_\alpha(q,p)$ induced by the transformation properties of q_k,p_k. Thus we find that J and J_2 in Eqs. (3) and (4) are invariant with respect to any C_n rotation of the (q_x,q_y) coordinate plane (the C_n axis is usually chosen to be axis z). Therefore J_2 can be labeled as J_z, a projection of J on the C_n axis. In practice, the quantity $2J_2$ is often called l, the "vibrational angular momentum" of the two-mode axially symmetric system.[18] The representation spanned by $(J_2=J_z,J_1,J_3)$ is $(A_2' \oplus E')$ (the J_2 component has the A_2 symmetry) and the group image in this representation is D_3; this is the group that should be used in the *reduced* phase space.

Thus the two-mode problem with J=const, i.e., with the SU(2) dynamical symmetry, is equivalent to an effective rotational problem [up to the well-known homomorphism $SU(2) \to SO(3)$].[19,20] In particular, the reduced phase space of this two-mode problem is the same as the classical phase space of the rotational problem, a two-dimensional sphere S_2, often called a polyad phase sphere[21–23] (note that $CP_1 \cong S_2$). Therefore, we consider a familiar problem of the stationary points of a classical Hamiltonian function, an energy surface,[24] defined on S_2.

The only important point to stress is that in the *simplest* possible case, which is the case near the equilibrium, the set of possible stationary points of such a function is entirely defined by the action of a particular group, namely the image of the molecular symmetry group in the (J_1,J_2,J_3) representation, on the S_2 space and by the topology of S_2. This set corresponds to the set of nonlinear normal modes of the initial problem.

Thus the action of the D_3 group on the polyad phase space is identical to the natural action of this group on the sphere and has three (isolated) critical orbits with the isotropy groups C_3, C_2, and C_2' (the D_3 group has two nonconjugating C_2 subgroups). The numbers of equivalent points in each orbit are 2, 3, and 3, respectively. It proves that a generic, or Morse function[25] which has (eight) stationary points *only* on these critical orbits can exist in the S_2 topology.[15] Moreover, since the two C_3 stationary points must be stable[26] there are three equivalent stable C_2 points, while three others are unstable as prescribed by the topology of the S_2 space.[15] Consequently, the only "choice" a particular system may have is between the $E(C_3) > E(C_2') > E(C_2)$ or $E(C_3) < E(C_2') < E(C_2)$ arrangements of the energies of the stationary solutions.

The stationary points of the simplest Hamiltonian on the reduced phase space and the periodic trajectories of the initial system near the equilibrium correspond. The isotropy symmetry group is the guide to this correspondence. Thus, the two C_3 points correspond to the $\Pi_{7,8}$ modes with the same isotropy symmetry group. The two triads of stationary points with the C_2 and C_2' isotropy groups correspond to the two families of equivalent periodic trajectories, $\Pi_{1,2,3}$ and $\Pi_{4,5,6}$, with the C_s and C_s' isotropy groups.[27] Here we retain the notation used in the analysis of the Hénon–Heiles Hamiltonian.[7,3]

There are two properties of nonlinear normal modes which deserve particular attention in molecular applications: their stability and their configuration space image. Again, these properties (of nonlinear normal modes) are generic and can be predicted without any analysis of a particular nonlinear Hamiltonian.

If we consider a coordinate plane (q_x,q_y) the classically allowed region for any energy E=const can be represented on it by a deformed circle, invariant with respect to the C_{3v} group.[27] As shown in Fig. 1 the two $\Pi_{7,8}$ periodic trajectories lie within this region and have a similar closed curve shape since they remain invariant under the C_3 operation. Moreover, since these trajectories are equivalent they can be transformed into each other by any of the σ_v reflections. This is similar to the two corresponding stationary points on the polyad phase sphere (two poles of S_2) being interchanged by any of the C_2 rotations. We conclude that Π_7 and Π_8 must therefore coincide in space but differ in time evolution, shown by arrows in Fig. 1.

Similar simple considerations give the image of the C_2-invariant trajectories. They form two qualitatively different triads of equivalent degenerate periodic trajectories. The degeneracy, i.e., that the trajectory image in the coordinate plane consists of a line with the turning points at the border of the classically allowed region, follows from the C_2 invariance. As shown in Fig. 1 one triad, $\Pi_{1,2,3}$, can be placed on the three C_2 axes, and another, $\Pi_{4,5,6}$, in a general position. It can also be shown[15] that $\Pi_{4,5,6}$ should be intermediate in energy and thus be unstable.

We conclude that a D_{3h} symmetric triatomic molecule near equilibrium has two different types of stable bending vibrations. For the same value of the approximate integral of the motion J=const these two periodic motions lie at the opposite ends of the corresponding energy region. The "circular" $\Pi_{7,8}$-type vibrations form a double degenerate nonlinear normal mode and correspond to a collective rotation of the three nuclei around their equilibrium positions.[28] The $\Pi_{1,2,3}$ periodic trajectories form a triply degenerate nonlinear normal mode. Its visualization in Fig. 1 shows that a single valence angle is predominantly deformed for each of the three classical trajectories. Therefore such a mode may be called a *local bending mode.*

Nonlinear normal modes provide a qualitative insight into the dynamics of the system and, in particular, into mode localization phenomena at low energies. To visualize these phenomena we can use the classical trajectory calculations for the Hénon–Heiles Hamiltonian.[29–31] Regular trajectories, precessing and librating, "coil" around the stable periodic trajectories, $\Pi_{7,8}$ and $\Pi_{1,2,3}$ (cf. Refs. 29 and 30). They correspond to the precession of **J** around the C_3

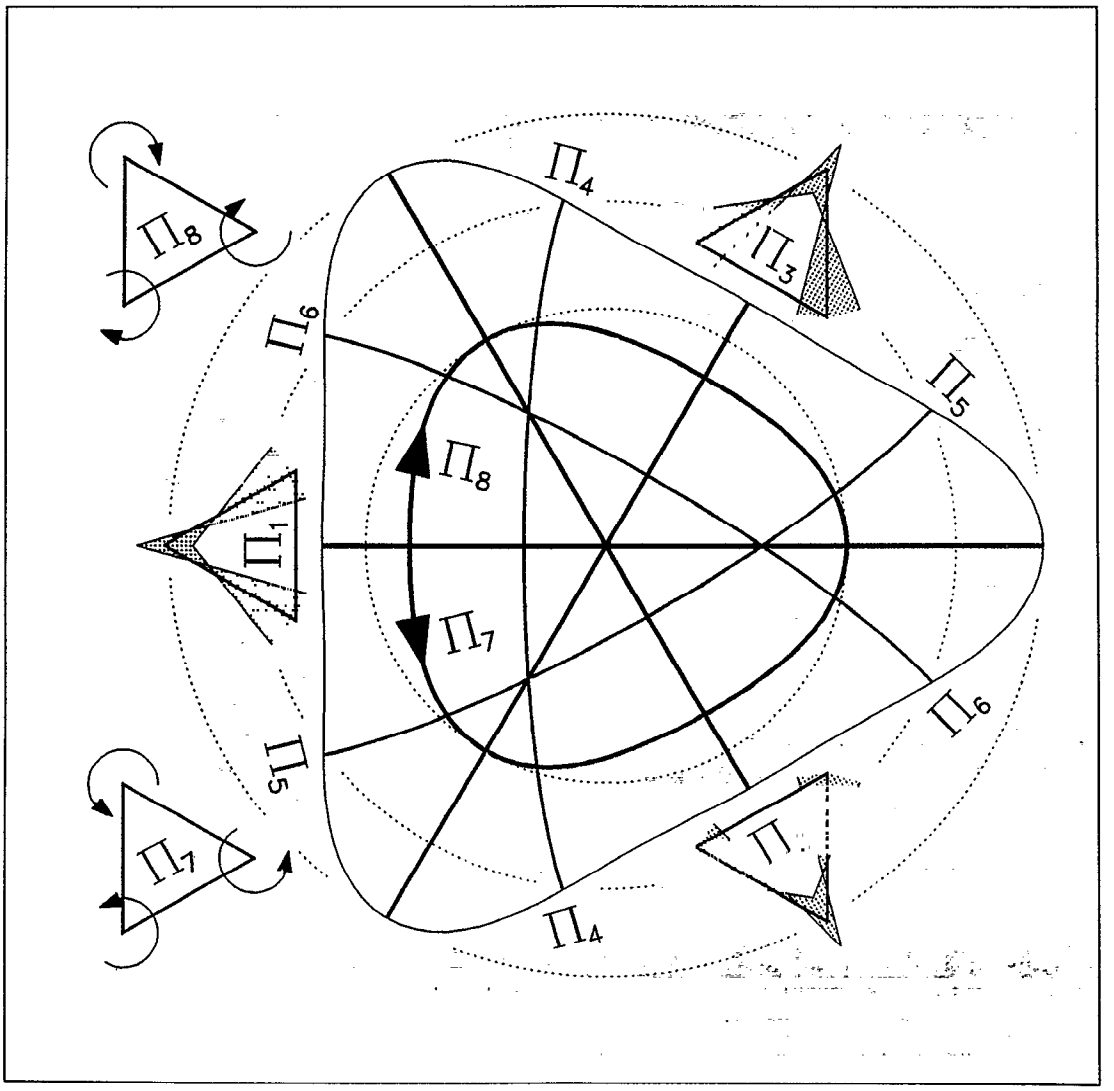

FIG. 1. Nonlinear normal modes of a D_3-symmetric 2D oscillator and the bending vibrations of a D_{3h} symmetric triatomic molecule.

axis, and each of the three C_2 axes (cf. Fig. 7 of Ref. 31). We note that the $\Pi_{7,8}$ modes are common to any axially symmetric system: J_z (or l) is nearly conserved, whereas the $\Pi_{1,2,3}$ modes are specific to our problem: we should consider the projection of J on one of the three C_2 axes. Irregular, or chaotic, trajectories are close in energy to $\Pi_{4,5,6}$, and tend to occupy the entire potential well.[30,31] They lie in the vicinity of the separatrix on the polyad phase sphere.

B. Three-mode case: $\nu_2(E')$ and $\nu_1(A_1')$

The treatment of the full three-dimensional (3D) vibrational Hamiltonian brings essentially no new information in the nonlinear normal mode analysis. Indeed, since the third coordinate under consideration is totally symmetric, the nontrivial action of the symmetry group is simply that on the $\nu_2(E')$ subspace discussed in the preceding section.

A formal scheme of analysis would be as follows. Consider the Hamiltonian functions defined over the CP_2 reduced phase space.[13] The action of the D_3 group (the image of D_{3h} in the space of all bilinear combinations $a_\alpha^+ a_\beta$, $\alpha,\beta=2x,2y,1$ is D_3) on this space is given in detail by Zhilinskiĭ in Fig. 3 and Table II of Ref. 13. We summarize these results in Table I. The only critical orbit associated with the $\nu_1(A_1)$ vibration is Π_0. It is isolated and stable. The corresponding periodic trajectory is degenerate, and its image in the 3D coordinate space ($q_{2x},q_{2y},q_1=z$) lies on axis z (the classically allowed region of the coordinate space in this case is a C_{3v} invariant closed surface, a deformed sphere).

As seen from Table I, the stationary points of the simplest Morse Hamiltonian lie not only on the critical orbits of the group action: The $\Pi_{7,8}$ and $\Pi_{4,5,6}$ stationary points lie on critical orbits, whereas the $\Pi_{1,2,3}$ points do not.[32] The $\Pi_{1,2,3}$ points are no longer fixed in phase space, but can move (on the surfaces of the three equivalent spheres) if,

TABLE I. Action of the D_3 group on the CP_2 reduced phase space of the $\nu_2(E)+\nu_1(A_1)$ polyads of a D_{3h} symmetric triatomic molecule (after Ref. 13).[a]

Isotropy group	Orbit	Type of orbit	Stationary point(s)
D_3	1 point	critical	Π_0
C_3	2 points	critical	$\Pi_{7,8}$
C_2^a	3 points	critical	$\Pi_{4,5,6}$
C_2^b	3 points	noncritical	$\Pi_{1,2,3}$

[a]Note: a,b stand for the two nonconjugating C_2 subgroups of D_3.

for example, the polyad number J changes. Figure 1 may be treated as representing the projections of the $\Pi_{7,8}$, $\Pi_{1,2,3}$, and $\Pi_{4,5,6}$ 3D trajectories on the (q_{2x},q_{2y}) plane of bending coordinates. The trajectories themselves can come out of this plane as ν_2 mixes with ν_1. However, since $\sigma_v(\Pi_7)=\Pi_8$, the 3D configuration space images of the two "circular" modes still coincide. On the other hand, the degeneracy of the $\Pi_{1,2,3}$ trajectories may not persist, since they are located in the σ_v planes and no operation of the C_{3v} group changes their time evolution property. Thus the actual images of $\Pi_{1,2,3}$ might not reach the boundary of the classically allowed region. It is interesting to understand the relation between the changes these trajectories can undergo remaining in the three σ_v planes, such as a transition from a degenerate to a nondegenerate trajectory, and the position of the $\Pi_{1,2,3}$ stationary points on the three C_2 invariant spheres of the reduced phase space (on the continuous S_2 part of the C_2 stratum, see Fig. 3 of Ref. 13). Conversely, the $\Pi_{4,5,6}$ trajectories remain degenerate.[33] It is equally interesting to mention that the broken degeneracy is associated in this case with the broken σ_v symmetry ($\Pi_{4,5,6}$ stationary points lie on the isolated orbit—any departure from this point breaks the C_2 symmetry).

C. Quantum-classical correspondence

There are two aspects in the quantum problem which can be qualitatively understood on the basis of the classical trajectory analysis: patterns in the energy level spectrum, such as regular sequences of levels, or clusters, i.e., groups of quasidegenerate levels, and corresponding localization patterns of quantum wave functions (cf. the broad discussion on these topics in the Hénon–Heiles literature[30,34,35]). Both are associated with the existence of stable periodic trajectories in the classical problem. Thus, at low energies we may expect three different regular groups of quantum states: Those localized near Π_0 are just overtones of the ν_1 mode, those localized near $\Pi_{7,8}$ form l doublets, and the last but not the least are those which are localized near $\Pi_{1,2,3}$ and form quasidegenerate triplets.

The $\Pi_{1,2,3}$ type states, or local bending states, are, perhaps, the most interesting. The vibrational angular momentum (3) in these states has a small projection $l=2J_z$ on the C_3 axis and is quantized along one of the C_2 axes. The vibrational energy levels form $A+E$ clusters, e.g., $4^0A_1+4^2E$, or $5^1E+5^3A_1$, where we use the conventional $N^l\,\Gamma$ labels of vibrational states. Of course, the l label for these states has very little physical meaning. To better visualize the localization of corresponding quantum wave functions, one should build three equivalent combinations $\theta_{1,2,3}$ of the symmetrized wave functions $|E_x\rangle$, $|E_y\rangle$, and $|A_1\rangle$ as follows:[36]

$$\theta_1=\frac{1}{\sqrt{2}}\,(|A_1\rangle+|E_x\rangle),$$

$$\theta_{2,3}=\frac{1}{\sqrt{2}}\,(|A_1\rangle-\frac{1}{2}\,|E_x\rangle\pm\frac{\sqrt{3}}{2}\,|E_y\rangle). \tag{5}$$

Functions $\theta_{1,2,3}$ cannot be the eigenfunctions of the problem; however, the subspace spanned by the three wave functions can be equivalently represented by such mode localized functions.[37] Such a representation is physically meaningful if the corresponding eigenvalues are (nearly) degenerate. If localization near $\Pi_{1,2,3}$ occurs, then $\theta_{1,2,3}$ will be localized near each of the C_2 axes in the (q_{2x},q_{2y}) coordinate plane. Moreover the images of the node planes of $\theta_{1,2,3}$ in the coordinate plane would be orthogonal to the C_2 axes, so that for given N every $\theta_{1,2,3}$ function would have N nodes on its stability axis C_2.

The quantum analogs of the $\Pi_{7,8}$-type, or "circular," motion can be best understood by an analogy to the well-known eigenfunctions of the isotropic (C_∞ symmetric) 2D oscillator.[38] We are particularly interested in the $l=N$ states since they are most prominently localized near the $\Pi_{7,8}$ trajectories. Indeed, the radial part of the $l=N$ wave functions has only one maximum and the angular dependence is $\cos(N\varphi)$ for "even" functions and $\sin(N\varphi)$ for "odd" functions, so that they look like "$2N$-petal daisies." Of the even–odd pair of the eigenstates of l^2, we can construct "circular" states with the angular part $\exp(\pm N\varphi)$. The latter are the eigenstates of l: The projection of $\mathbf{J}$ on axis z, $2J_z=l$, is well defined so that these states correspond to the counterclockwise and clockwise, Π_7 and Π_8, circular motions. Breaking symmetry down to D_3 results in a corresponding distortion of the "daisies." Again, from an even–odd pair of l-doublet eigenfunctions we can construct two "circular" states:

$$(\psi'_\mp)^*=\psi'_\pm=\begin{cases}\dfrac{1}{\sqrt{2}}\,(|A_1\rangle\pm i|A_2\rangle), & l=3,6,\ldots\\[2ex] \dfrac{1}{\sqrt{2}}\,(|E_x\rangle\pm i|E_y\rangle), & l\neq 3,6,\ldots.\end{cases} \tag{6}$$

We note, that in the $l=3,6,\ldots$ case the two complex wavefunctions $\psi'_{7,8}$ (6) have exactly the symmetry of the $\Pi_{7,8}$ trajectories. However, for the sake of visualization it is more convenient to use two equivalent real "daisy" functions with the symmetry properties of $\Pi_{7,8}$:

$$\theta_{7,8}=\frac{1}{\sqrt{2}}\,(|A_1\rangle\pm|A_2\rangle), \tag{7}$$

such that "circular" states differ only by a constant phase:

$$\psi^*_\mp=\psi_\pm=\frac{1}{\sqrt{2}}\,(\theta_7\pm i\theta_8)=\psi'_\mp e^{\pm\pi/4}. \tag{8}$$

TABLE II. Calculated band origins, in cm^{-1}, for D_3^+ below the barrier to linearity. H_3^+ band origins from Ref. 8 are given for the same energy region.

State	Γ	(v_1,v_2^l)	v_1+v_2	D_3^+	H_3^+
1	A_1	$(0,0^0)$	0	0	0
2	E	$(0,1^1)$	1	1 835.1	2 521.3
3	A_1	$(1,0^0)$	1	2 301.2	3 178.3
4	A_1	$(0,2^0)$	2	3 530.7	4 777.0
5	E	$(0,2^2)$	2	3 651.2	4 997.4
6	E	$(1,1^1)$	2	4 060.0	5 553.7
7	A_1	$(2,0^0)$	2	4 554.6	6 262.0
8	E	$(0,3^1)$	3	5 214.0	7 003.4
9	A_1	$(0,3^3)$	3	5 400.6	7 282.5
10	A_2	$(0,3^3)$	3	5 470.0	7 492.6
11	A_1	$(1,2^0)$	3	5 712.1	7 769.1
12	E	$(1,2^2)$	3	5 795.7	7 868.6
13	E	$(2,1^1)$	3	6 236.5	8 487.0
14	A_1	$(3,0^0)$	3	6 760.7	9 251.5
15	A_1	$(0,4^0)$	4	6 772.9	8 996.6
16	E	$(0,4^2)$	4	6 858.5	9 107.6
17	E	$(0,4^4)$	4	7 169.2	9 996.5
18	E	$(1,3^1)$	4	7 368.3	9 650.6
19	A_1	$(1,3^3)$	4	7 452.2	9 964.0
20	A_2	$(1,3^3)$	4	7 535.1	10 208.4
21	A_1	$(2,2^0)$	4	7 830.8	10 592.1
22	E	$(2,2^2)$	4	7 892.5	10 642.6
23	E	$(0,5^1)$	5	8 295.6	10 853.3
24	E	$(3,1^1)$	4	8 364.9	11 321.5
25	A_1	$(0,5^3)$	5	8 372.5	10 913.1
26	A_2	$(0,5^3)$	5	8 599.7	11 525.4
27	E	$(1,4^2)$	5	8 789.2	11 651.1
28	A_1	$(1,4^0)$	5	8 863.4	11 809.2
29	A_1	$(4,0^0)$	4	8 919.8	12 145.9
30	E	$(0,5^5)$	5	9 030.7	12 073.2
31	E	$(1,4^4)$	5	9 162.3	⋯
32	E	$(2,3^1)$	5	9 423.1	
33	A_1	$(2,3^3)$	5	9 460.6	
34	A_2	$(2,3^3)$	5	9 553.4	
35	A_1	$(0,6^0)$	6	9 691.3	
36	E	$(0,6^2)$	6	9 726.1	
37	A_1	$(3,2^0)$	5	9 895.0	
38	E	$(3,2^2)$	5	9 941.2	
39	E	$(0,6^4)$	6	10 124.2	
40	A_1	$(1,5^3)$	6	10 265.3	
41	E	$(1,5^1)$	6	10 352.3	
42	A_2	$(1,5^3)$	6	10 406.5	
43	E	$(4,1^1)$	5	10 445.3	
44	A_1	$(0,6^6)$	6	10 668.8	
45	E	$(2,4^2)$	6	10 700.2	
46	A_2	$(0,6^6)$	6	10 798.0	
47	A_1	$(2,4^0)$	6	10 919.6	
48	E	$(1,5^5)$	6	10 962.0	
49	E	$(0,7^1)$	7	10 999.2	
50	A_1	$(0,7^3)$	7	11 014.7	
51	A_1	$(5,0^0)$	5	11 031.9	

III. LOCALIZED VIBRATIONAL STATES OF H_3^+ AND D_3^+

The H_3^+ molecular ion can be used as a natural and simple example of a real molecular system which has nontrivial vibrational behavior, such as localized bending vibrations, at arbitrarily low energies. However, the potential of H_3^+ has a low barrier to linearity ($\sim$12 000 cm^{-1} above the vibrational ground state[39]), so that only a few bending overtones, $N<6$, lie below this barrier while above it the polyad approximation itself rapidly deteriorates. Since at low polyad numbers quantum states cannot localize effectively we are confined to the analysis of the $N=4,5$ polyads. It is also natural to study the energy spectrum of a heavier isotopomer, D_3^+, for which the $N=4,5,6$ polyads can usefully be studied.

A number of calculations of pure vibrational energies of H_3^+ were recently reported.[8,40–42] All of them agree well (to within 0.1 cm^{-1}) in the energy range of interest. In this work we use H_3^+ energy levels and wave functions from the recent 3D discrete variable representation (DVR) calculations of Henderson, Tennyson, and Sutcliffe.[8] These calculations used scattering coordinates (r_1 is an H–H distance, r_2 the distance from the midpoint of r_1 to the third H, and θ is the angle between $\mathbf{r}_1$ and $\mathbf{r}_2$) and, for the results we show, a final Hamiltonian of dimension $N=6500$.

The scattering coordinate calculations are performed using C_{2v} rather than D_{3h} symmetry.[43] In this case the even calculation gives the levels of A_1' and E_x' symmetry and the odd one gives those of A_2' and E_y' symmetry.

D_3^+ calculations were performed using the 3D DVR program of Henderson and co-workers[8,44] and a final Hamiltonian of dimension $N=3500$. This is sufficient to converge all the energy levels in the region of interest, which are presented in Table II, to within 0.1 cm^{-1}.

The problem of assignment of low-lying levels of H_3^+ in terms of N^l was partially solved by Tennyson and Henderson by plotting node patterns of the wave functions.[40] These assignments were extended by Carter and Meyer whose hyperspherical coordinates are more convenient in this respect.[41] In Table III we list the energies of the vibrational polyads of H_3^+ and D_3^+. We note that these polyads do not overlap in energy; however, the validity of the N^l assignments above the barrier to linearity is arguable.[45]

TABLE III. Quasidegenerate vibrational triads in the structure of bending ($v_1=0$, $v_2=N$) polyads of H_3^+ and D_3^+. Band origins ω and energy gaps, $\Delta E=E(N^l)-E(N^{l-2})$, are given in cm^{-1}.

	H_3^+		D_3^+	
$N^l\Gamma$	ω	ΔE	ω	ΔE
$6^6\ A_2$	15 179[a]	516	10 798	130
$6^6\ A_1$	14 662[a]	1082	10 668	544
$6^4\ E$	13 580[a]	1286	10 124	398
$6^2\ E$	12 294[a]	−69	9 726	35
$6^0\ A_1$	12 363	⋯	9 691	⋯
$5^5\ E$	12 073	548	9 030	431
$5^3\ A_2$	11 525	612	8 599	227
$5^3\ A_1$	10 913	60	8 372	77
$5^1\ E$	10 853	⋯	8 295	⋯
$4^4\ E$	9 996	889	7 169	311
$4^2\ E$	9 107	111	6 858	85
$4^0\ A_1$	8 996	⋯	6 773	⋯
$3^3\ A_2$	7 492	210	5 470	70
$3^3\ A_1$	7 282	279	5 400	186
$3^1\ E$	7 003	⋯	5 214	⋯

[a]As assigned by Carter and Meyer (Ref. 41).

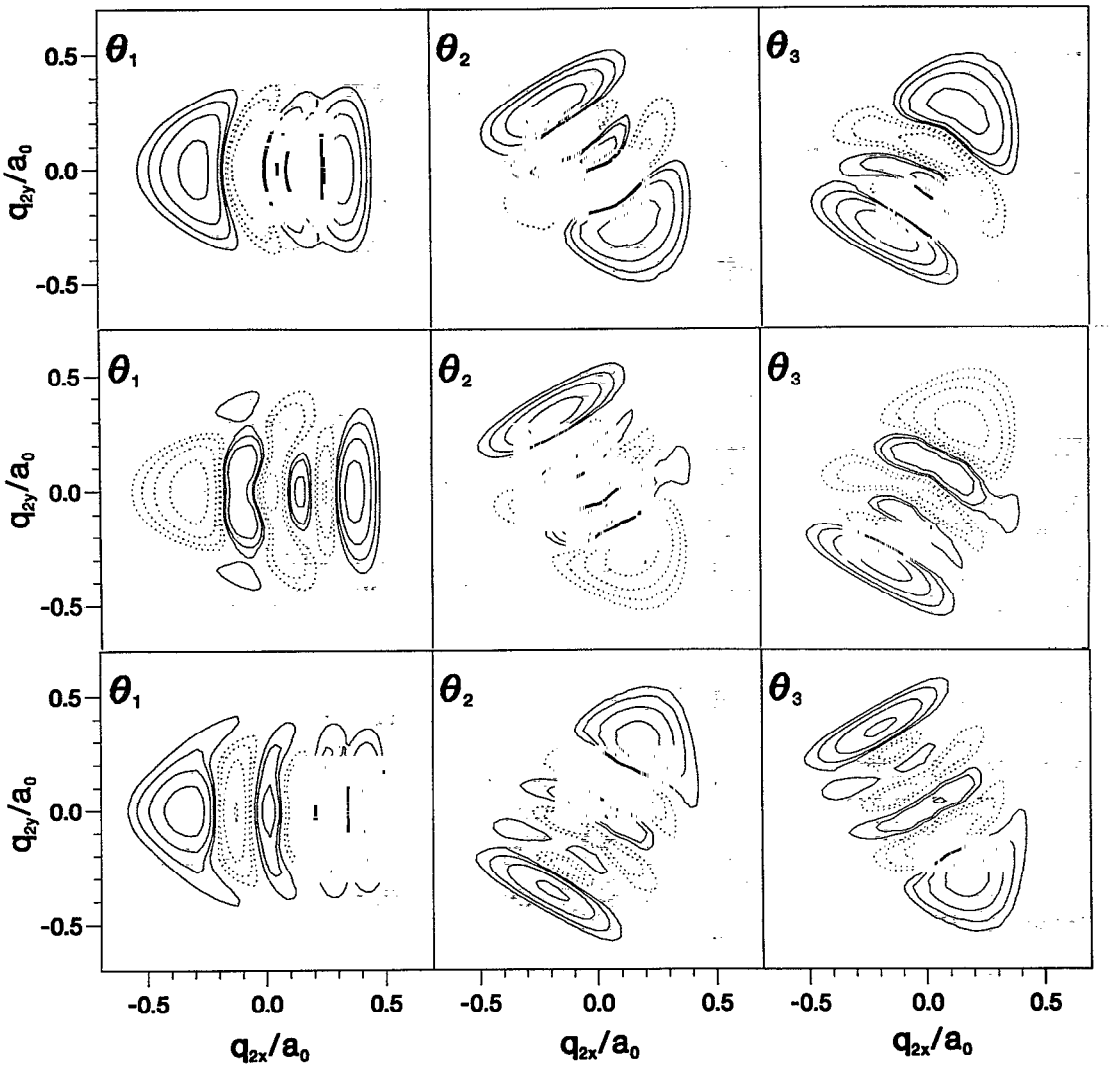

FIG. 2. Equivalent combinations $\theta_{1,2,3}$ of the low-l wave functions of D_3^+ showing the mode localization near the three equivalent C_2 axes. Combinations of $|0,4^0A_1\rangle$ and $|0,4^2E\rangle$ are shown in the upper row, of $|0,5^3A_1\rangle$ and $|0,5^1E\rangle$ in the middle row, of $|0,6^0A_1\rangle$, and $|0,6^2E\rangle$ in the bottom row. The number of nodes on the axes equals $N=4,5,6$.

It can be seen that the structure of the polyads corresponds to $E(\Pi_{7,8}) > E(\Pi_{4,5,6}) > E(\Pi_{1,2,3})$.

A. Localized bending states

The bending states localized near $\Pi_{1,2,3}$ can be recognized for $N=5$, 6, and, perhaps,[46] $N=4$, at low energies of each polyad as A_1+E clusters (see the distances between neighboring levels, ΔE, in Table III). Particularly characteristic is the near degeneracy of the 6^0 and 6^2 states and the splitting of the 5^3 levels, which is far larger than the energy gap between the lowest 5^1 E and 5^3 A_1 levels.

To obtain further evidence of the localization near $\Pi_{1,2,3}$ we analyzed the behavior of the wave functions corresponding to the low-l levels in Table III. Initial functions in the Jacobi coordinates (r_1,r_2,θ) were represented in the symmetrized displacement (from the D_{3h} equilibrium) coordinates (q_1,q_{2x},q_{2y}), and plotted at $q_1=0$ in the form of combinations $\theta_{1,2,3}$ in Eqs. (5).

Plotting 3D wave functions computed in scattering coordinates in another coordinate system, such as symmetrized displacement coordinates, is not straightforward. For this purpose we have developed programs which use 3D linear interpolation between DVR points to obtain the amplitude of the wave function at an arbitrary point. As the even and odd calculations were performed on slightly different DVR grids,[8] it is necessary to perform the interpolation prior to taking linear combinations of these functions.

The results, such as in Fig. 2, clearly show the expected localization pattern. At the same time the influence of the $\Pi_{4,5,6}$ type motion, in particular at low N, should probably be acknowledged. In principle, the combinations $\theta_{1,2,3}$ (for any A_1+E pair) should be (i) identical up to the C_3 rotation, and (ii) invariant with respect to a particular σ_v reflection. Since the wave functions we used are obtained in the basis symmetrized only according to the C_{2v} group,[40] only the $\sigma_v(x)$ symmetry properties are exactly respected

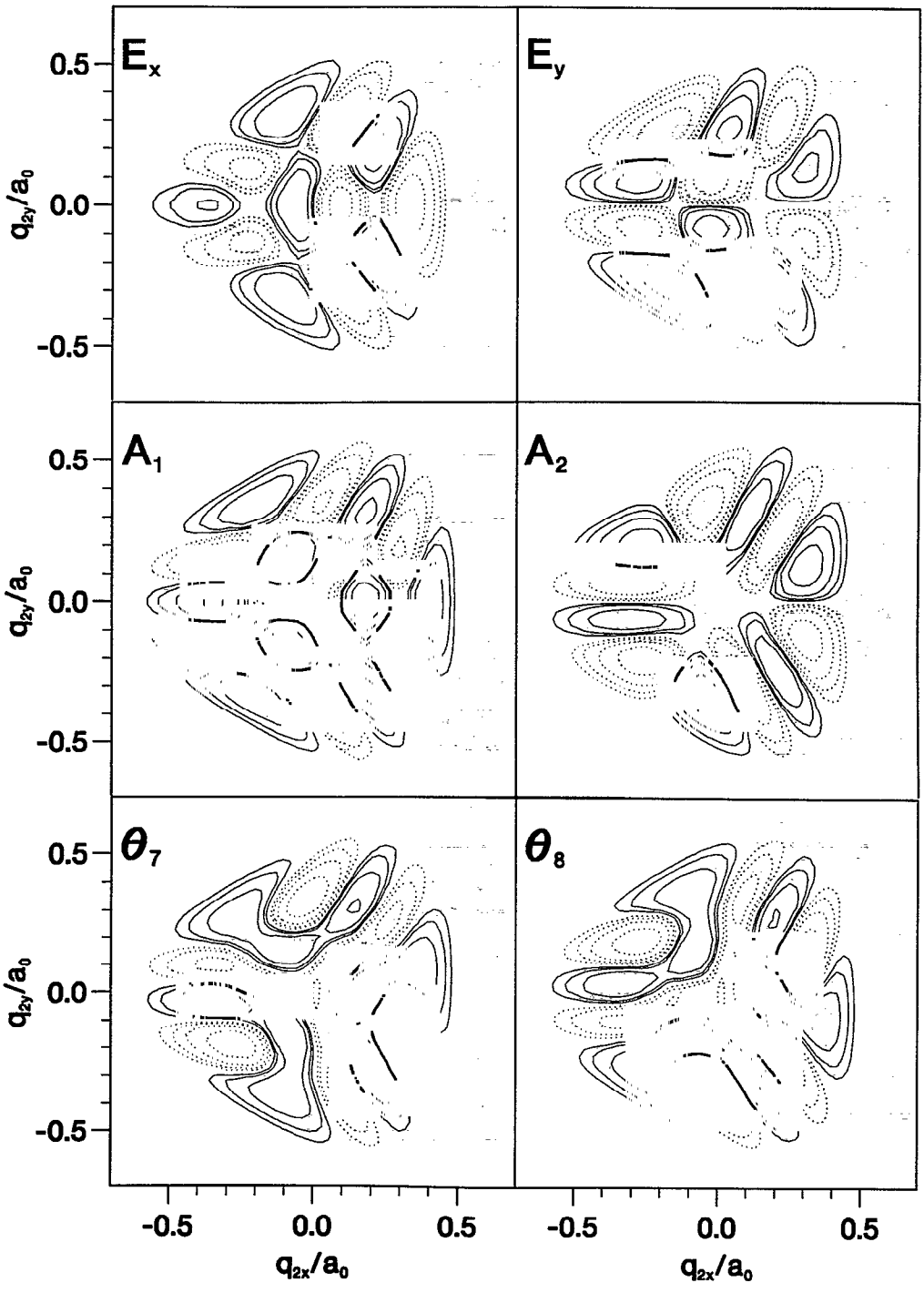

FIG. 3. Wave functions of the high $l=N$ states of D_3^+: $(0,5^5)E_x$ and E_y (top), $(0,6^6)A_1$ and A_2 (middle), equivalent combinations $\theta_{7,8}$ of the $(0,6^6)$ functions (bottom).

in our plots. Comparison of H_3^+ and D_3^+ wave functions shows that the mass of the molecule has little effect on the localization: Both the states of D_3^+ and H_3^+ are mode localized.

B. Circular states

As we discuss in Sec. II C, high-l bending states, especially the $l=N$ states, of D_3^+ and H_3^+ can be interpreted as quantum analogs of the $\Pi_{7,8}$-type classical motion. However, due to symmetry limitations only the $l=N=6$ states are best suited for such interpretation ($N=3$ is too low to fully observe the quantum-classical correspondence).

The $l=N$ states themselves, such as $(0,5^5)$ and $(0,6^6)$ states in Fig. 3, clearly show expected "circular" localization patterns with, respectively, 10 and 12 nodes on the $\Pi_{7,8}$ line. In the latter case we can actually construct the

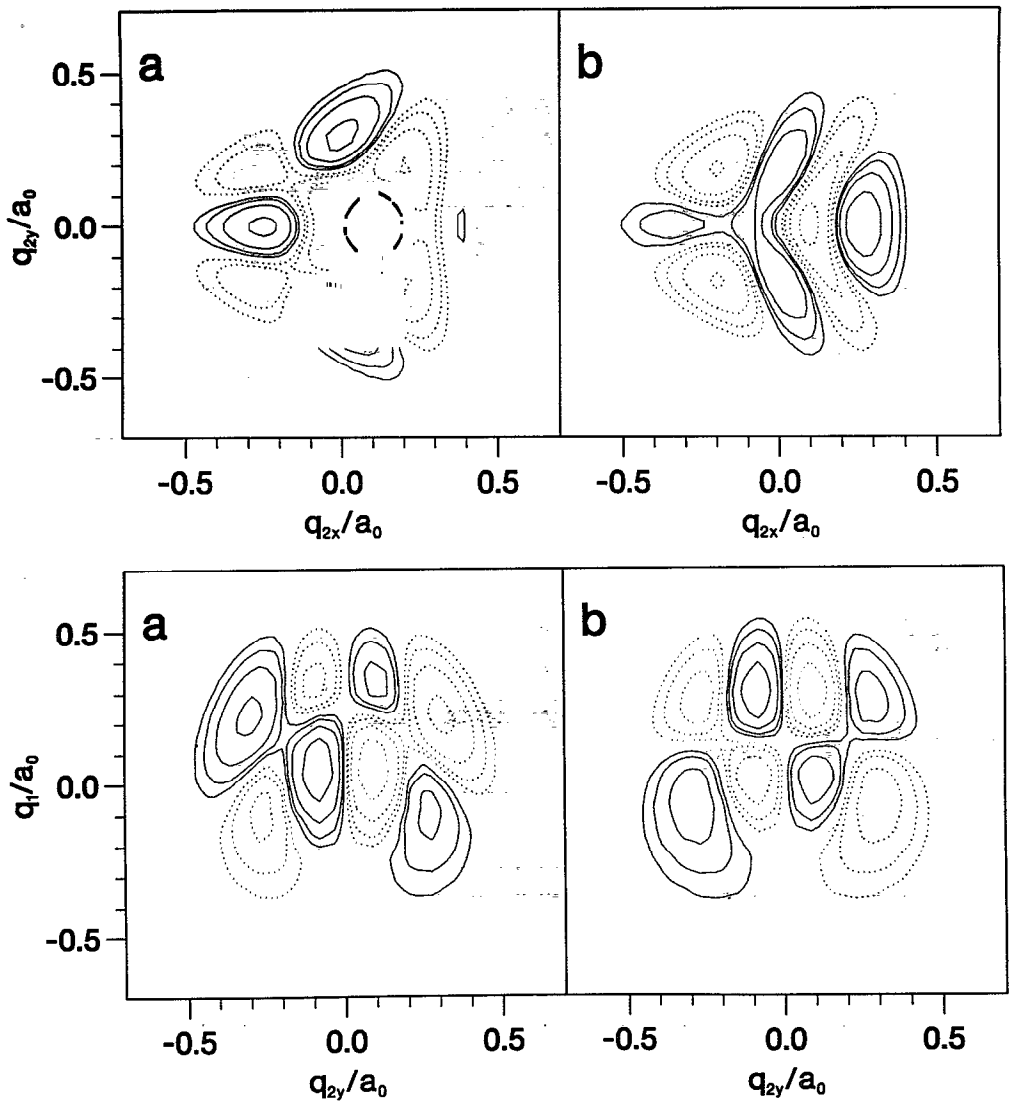

FIG. 4. The resonance between the $(0,4^4)E$ (left) and $(1,3^1)E$ (right) states of D_3^+: odd (E_y) components in the ($q_1=0,q_{2x},q_{2y}$) plane (top) and in the ($q_1,q_{2x},q_{2y}=0$) plane (bottom).

wave functions $\theta_{7,8}$ (7) with *exactly the same symmetry* as trajectories $\Pi_{7,8}$ in Fig. 1. They appear at the bottom of Fig. 3 as "right" and "left" C_3-symmetric "propellers."

We note that of the two states, A_1 and A_2, the odd state is higher in energy and less perturbed (there are few A_2 states in the spectrum and they are far apart), so that it exhibits a clearer circular localization. Comparing H_3^+ and D_3^+ (cf. Table III) we also conclude that, perhaps because they lie relatively deeper in the C_{3v} potential well, high-l states of D_3^+ show more prominent "circular" localization.

C. The 1:1 resonance of ν_1 and ν_2

Above we analyzed D_3^+ and H_3^+ wave functions in terms of noninteracting ν_1 and ν_2 vibrational modes and find mode localization of bending states, as predicted from a classical analysis. However, as noted in Sec. II B, to complete such an analysis the consequences of possible ν_1, ν_2 resonances should be considered. This involves studying other projections, such as q_1 vs q_{2x} or q_1 vs q_{2y}, of full 3D wave functions.[47]

One of the features we observed this way is mixing of high-l bending states with close-lying "breathing" states such that $\Delta v_1=-\Delta v_2=1$. In general, this 1:1 resonance of the $\nu_1(A_1)$ and $\nu_2(E)$ modes can be ascribed only to quartic anharmonic terms while the 1:2 (Fermi) resonance is caused by cubic terms. However, spacing between the levels coupled by the 1:1 (quartic) terms can be very small and consequently significant mixing of these states occurs. Thus the simple three-mode polyad model and the analysis in Sec. II B find certain confirmation. Moreover, at higher energies (see $N=6$ in Table II) it also appears that major mixing occurs for the states of the same polyad: $\Delta v_1=-\Delta v_2=1,2$, as can be described by different quartic terms of the same order of magnitude.

A particularly strong mixing of the states in D_3^+ assigned as $(0,4^4)$ and $(1,3^1)$ in Table II is illustrated in Fig. 4. In this case mixing is nearly 50% so that we can reconstruct the "pure" $(0,4^4)$ and $(1,3^1)$ components by simply taking $\pm$ combinations of the computed eigenfunctions. Indeed as shown in Fig. 5, this produces a clear $4\,^4E$ "circular" state with eight "petals" (cf. Fig. 3), while another combination is a clear $(1,3^1)$ state, and is a part of an $E+A_1$ triad (not shown). Therefore, as predicted in Sec. II B, we observe the same basic localization patterns.

The resonances of the above kind also contribute to the dynamics of lower states. Thus, for example, in the case of $(0,3^3)A_1$ we need to consider a contribution (of, to our estimate, as high as 20%) by the nearby $(1,2^0)A_1$. The role of resonances increases for higher states, such as $(0,6^6)A_1$.

IV. DISCUSSION

The analysis of low-lying excited bending vibrational states of H_3^+ and D_3^+ gives a clear illustration of the localized and circular vibrational bending states. These states correlate with the nonlinear normal modes, the periodic trajectories of the system near the equilibrium.

In general the mode localization we observe can be due to different reasons:

(i) Anharmonicity of the "static" 2D potential in the (q_{2x},q_{2y}) bending coordinates. One should note that such "static" potential, obtained as a section of the full 3D potential[39] at the equilibrium value of the ν_1 coordinate, is highly isotropic—its threefold symmetry is clearly seen only near the barrier to linearity. Hence the anharmonicity of this potential itself may not be the major cause for localization, as it is, for example, for a Hénon–Heiles potential. Such a conclusion is also supported by the extent to which the quantum wave functions spread over the area, classically allowed by the "static" 2D potential.

(ii) Anharmonicity of the "dynamic" 2D potential of

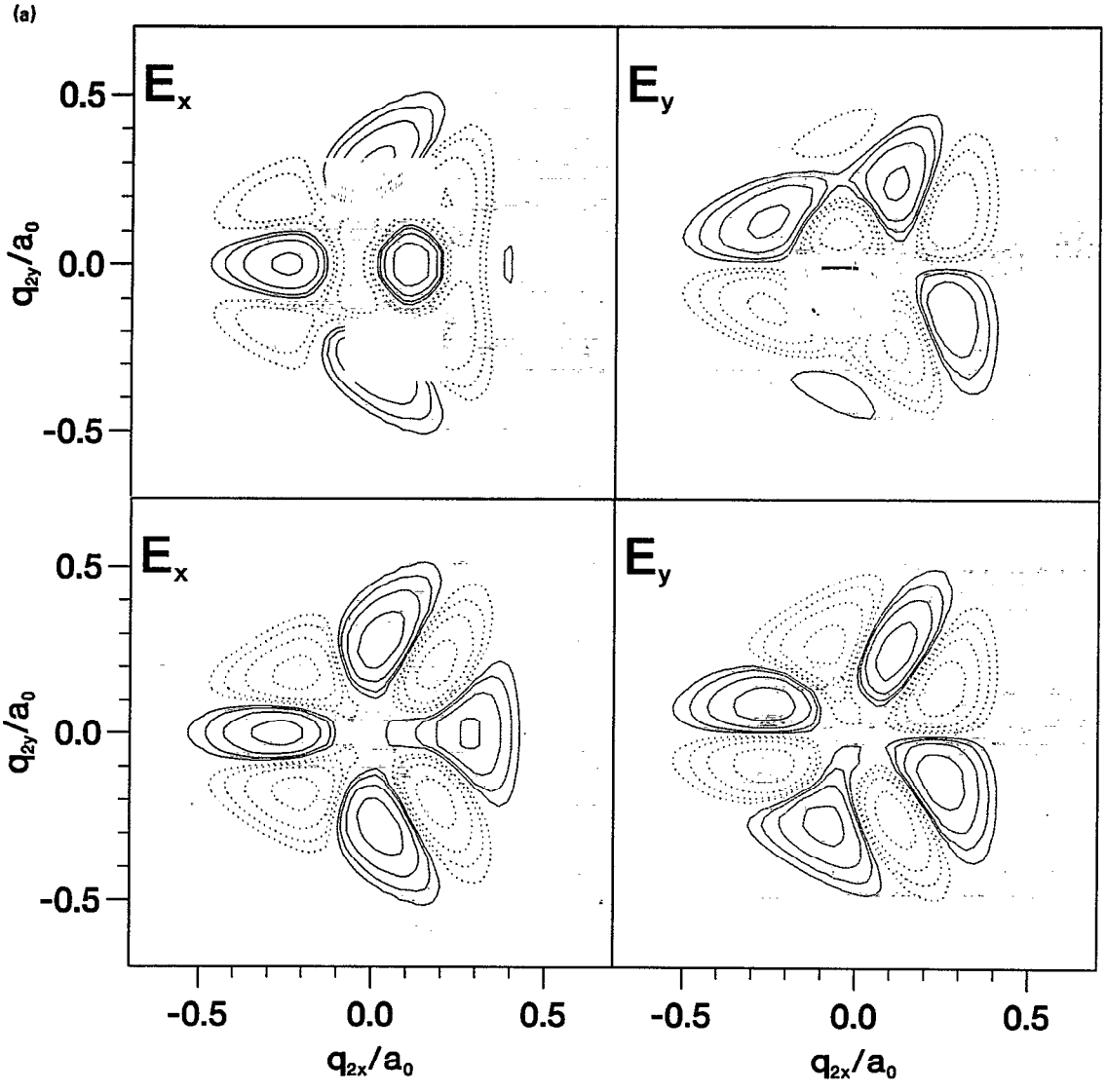

FIG. 5. Mixed states of D_3^+ assigned as $(0,4^4)$ (top part) and $(1,3^1)$ (bottom part). Eigenfunctions are shown in the first row of each part. Combinations $(0,4^4)+(1,3^1)$ and $(0,4^4)-(1,3^1)$, which display "pure" 4^4 and 3^1 behavior, are shown in the lower row.

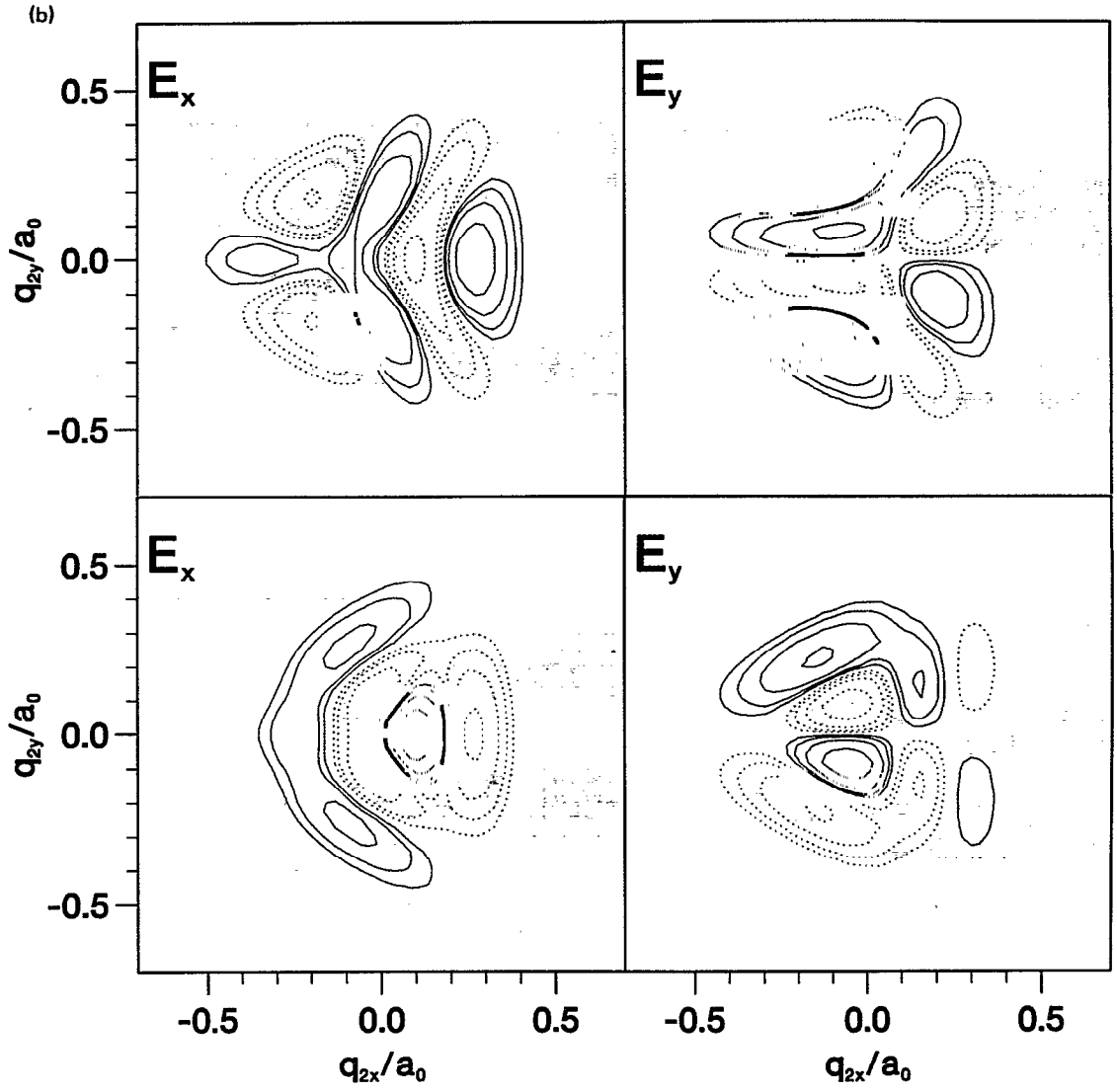

FIG. 5. (*Continued.*)

the bending mode which effectively takes mixing of ν_1 and ν_2 and the influence of the domain of highly excited states into account. More rigorously, we should speak of an effective 2D Hamiltonian, the one we actually imply in Sec. II A. In this case ν_1 and ν_2 are still nearly separable, i.e., v_1 and v_2, the number of quanta in each mode, are still good quantum numbers. This mechanism can be dominant unless strong resonances of ν_1 and ν_2, such as described in Sec. III C, occur.

(iii) Anharmonicity of the full 3D potential is such that ν_1 and ν_2 are (generally) nonseparable but the 3D Hamiltonian is in some sense "simple": its set of principal periodic trajectories is qualitatively the same as that of the system near linearization. The latter is the set of nonlinear normal modes we obtain in Sec. II B. One of these nonlinear modes, Π_0, is totally symmetric with respect to the C_{3v} group and coincides with ν_1 in the configuration space, so that for the states localized near the Π_0 trajectory $v_1 \gg v_2$ and ν_1 and ν_2 are nearly separable. This does not generally hold for other nonlinear normal modes since corresponding trajectories may significantly come out of the ν_2 plane. On the other hand, their projections in this plane are similar to the nonlinear normal modes of the 2D problem, so that similar mode localization patterns can be expected in these projections. An essential feature in this case is the existence of (at least) one approximate integral of the motion, the one the problem possesses near linearization. Table II and the analysis of resonances in Sec. III C indicate[45] that the classical action of the form (1) can well play the role of such integral, so that $N=v_1+v_2$ may be considered as a good quantum number, sometimes called a "superpolyad number."[48]

(iv) Dynamical mixing with highly excited states including those lying above the barrier to linearity

is essential. It seems, however, unlikely that the $N=v_1+v_2$ polyad approximation completely breaks down[11] for the states we consider. Rather we deal with a "dynamic" 3D and 2D potentials, or effective Hamiltonians which can implicitly account for other states within this approximation.

We conclude that vibrational mode localization in H_3^+ and D_3^+ is a complex, essentially three-mode effect. A great number of vibrational states of D_3^+ and H_3^+ can be qualitatively understood in terms of dynamics with at least one approximate integral of motion, $N=v_1+v_2$, so that conventional "assignments" remain valid even at fairly high energies.[47] This phenomenon of regularity, or quasiperiodicity, was to some extent discussed and understood.[30,34,35] In this context a 3D semiclassical study with the H_3^+ potential[39] is of great interest. In particular, the manifestation of unstable $\Pi_{4,5,6}$ trajectories and of their long-term regular behavior[31] may be better understood in such a study.

Another interesting problem is a further study of possible polyad, or SU(3) dynamical symmetry approximation used[11] in Sec. II B, and a closely related problem of vibrational resonances briefly discussed in Sec. III C (cf. Ref. 48).

ACKNOWLEDGMENTS

We thank Ruth Le Sueur for helpful comments on assignments. J. R. H. thanks the SERC for a Fellowship. Analysis of the wave functions was performed on an IBM RS/6000 under SERC Grant No. GR/G01874. D.S. thanks the Institute for Theoretical Atomic and Molecular Physics at Harvard University and Smithsonian Astrophysics Observatory for hospitality. This paper is issued as N. R. C. C. No. 34661.

[1] E. B. Wilson, J. C. Decius, and P. C. Cross, *Molecular Vibrations* (McGraw-Hill, New York, 1955).
[2] J. Tennyson, O. Brass, and E. Pollak, J. Chem. Phys. **92**, 3005 (1990); J. Chem. Phys. **92**, 3377 (1990).
[3] J. Montaldi, M. Roberts, and I. Stewart, Philos. Trans. R. Soc. London Ser. A **325**, 237 (1988); in *The Physics of Structure Formation*, edited by W. Güttinger and G. Dangelmayr (Springer, Berlin, 1987), p. 354.
[4] R. T. Lawton and M. S. Child, Mol. Phys. **37**, 1799 (1979); Ch. Jaffé and P. Brumer, J. Chem. Phys. **73**, 5646 (1980); M. S. Child and L. Halonen, Adv. Chem. Phys. **57**, 1 (1984); I. M. Mills and A. G. Robiette, Mol. Phys. **56**, 743 (1985).
[5] K. Stefanski and E. Pollak, J. Chem. Phys. **87**, 1079 (1987), and references therein. These authors discuss the periodic trajectories for two quasidegenerate stretching modes of ABA molecules (see their Figs. 1 and 2), and the H_2O-type bifurcation of the periodic trajectory associated with the symmetric stretch.
[6] M. Hénon and C. Heiles, Astronom. J. **69**, 73 (1964).
[7] R. C. Churchill, G. Pecelli, and D. L. Rod, in *Como Conference Proceedings on Stochastic Behavior in Classical and Quantum Hamiltonian Systems*, edited by G. Casati and J. Ford, Vol. 93 in Lecture Notes in Physics (Springer, Berlin, 1979), p. 76; D. L. Rod and R. C. Churchill, in *Singularities and Dynamical Systems*, edited by S. N. Pnevmatikos (Elsevier, New York, 1985), p. 385.
[8] J. R. Henderson, J. Tennyson, and B. T. Sutcliffe, J. Chem. Phys. **98**, 7191 (1993).
[9] J. Montaldi, M. Roberts, and I. Stewart, Nonlinearity **3**, 695 (1990); **3**, 731 (1990).
[10] In general, dynamical symmetry of a system near a stable-in-the-linear-approximation equilibrium point can be derived from the normal form of its Hamiltonian. The normal form theorem, initially proven by Birkhoff for nonresonance systems, can be appropriately modified in the case of resonances.
[11] A matrix classical Hamiltonian might be an extension of the polyad approach to higher energies, e.g., the nearest-neighbor approximation to polyad coupling.
[12] It is natural to consider the construction of CP_{n-1} in a complex space $C_n: z_k = (I_k)^{1/2}e^{i\theta_k}$. For a quantum nD oscillator CP_{n-1} can be obtained as a classical limit manifold.
[13] B. I. Zhilinskiĭ, Chem. Phys. **137**, 1 (1989). The action of several point groups, such as C_2, D_2, D_3, D_4, and O, on CP_2 (three-mode case) is analyzed here in detail.
[14] The finite invariance symmetry group of the Hamiltonian is essential for the present discussion since critical manifolds and corresponding nonisolated stationary solutions (may) exist in the case of continuous symmetry. See also Ref. 15.
[15] D. A. Sadovskiĭ and B. I. Zhilinskiĭ, Phys. Rev. A **47**, 2653 (1993).
[16] The full symmetry group acting on periodic trajectories involves both the image of the molecular symmetry group and the operations of time reversal and translation. The role of the latter operations can be seen from the discussion of Fig. 1.
[17] J. Schwinger, in *Quantum Theory of Angular Momentum*, edited by L. C. Biedenharn and H. van Dam (Academic, New York, 1965), p. 229.
[18] The name "angular momentum l" comes from the definition: $l=\mathbf{p}\times\mathbf{q}$, where $\mathbf{p}=(p_x,p_y,0)$ and $\mathbf{q}=(q_x,q_y,0)$.
[19] B. I. Zhilinskiĭ, *Theory of Complex Molecular Spectra* (Moscow University, Moscow, 1989) (in Russian).
[20] M. E. Kellman, J. Chem. Phys. **83**, 3843 (1985); W. G. Harter, *ibid.* **85**, 5560 (1986).
[21] R. Cushman and D. L. Rod, Physica D **6**, 105 (1982).
[22] V. B. Pavlov-Verevkin and B. I. Zhilinskiĭ, Chem. Phys. **128**, 429 (1988).
[23] L. Xiao and M. Kellman, J. Chem. Phys. **90**, 6086 (1989). Stretching polyads, $2J=v_1+v_3$, of H_2O have been studied in detail by S. E. Choi and J. C. Light, J. Chem. Phys. **97**, 7031 (1992), Figs. 2 and 3. See also Ref. 15.
[24] W. G. Harter and C. W. Patterson, J. Chem. Phys. **80**, 4241 (1984); W. G. Harter, in *Group Theoretical Methods in Physics*, edited by R. Gilmore (World Scientific, Singapore, 1987), p. 1; J. M. Robbins, S. C. Creagh, and R. G. Littlejohn, Phys. Rev. A **39**, 2838 (1989).
[25] A generic, or Morse function is smooth and possesses only nondegenerate isolated stationary points. Any sufficiently small variation of such a function results in a function with the same set of stationary points.
[26] A nondegenerate stationary point on a 2D manifold is necessarily stable (has Morse index 0 or 2) if its local symmetry group includes an m-fold axis, $m>2$.
[27] Any image of a group of transformations of a 3D space in a two-dimensional representation is in fact a group of transformations of a 2D space. The standard notation for such groups uses symbols D_1, D_2, D_3, etc. rather than C_s or C_{1v}, C_{2v}, C_{3v}, etc. However, since this notation might cause confusion in our context we use the latter, or 3D, notation. Therefore symbols C_{3v} and D_3, when denoting a 2D group, are simply identical. Moreover, we denote the rotation around an in-plane axis by C_2, while a proper 2D notation would be D_1. In the 3D case D_3 and C_{3v} denote different groups, namely the images of the D_{3h} group in the J representation, and in the q representation. The simple correspondence between the isotropy groups of stationary points and periodic trajectories is based on $D_3 \sim C_{3v}$.
[28] See also Ref. 1, Figs. 2 and 3.
[29] Ch. Cerjan and W. P. Reinhardt, J. Chem. Phys. **71**, 1819 (1979). Figures 5(a)–5(c) show the three kinds of classical trajectories of the Hénon–Heiles system at low energies.
[30] G. Hose, H. S. Taylor, and Y. Y. Bai, J. Chem. Phys. **80**, 4363 (1984). Figure 2 shows three types of quantum eigenfunctions of the Hénon–Heiles Hamiltonian, called Q^{I}, N, and Q^{II} which then are compared with classical trajectories near $\Pi_{7,8}$ (precessing), $\Pi_{4,5,6}$ (irregular), and $\Pi_{1,2,3}$ (librating) in Fig. 3. The Q^{I} and Q^{II}, or "quasiperiodic" states correspond to our "circular" and "localized bending" states. They are compared to the eigenfunctions of an isotropic 2D oscillator, and to that of a linear oscillator along one of the $\Pi_{1,2,3}$ directions. In the latter case the authors do not pay attention to the fact of clustering of Q^{II} levels into $A+E$ triads [well seen from their energy level data (Ref. 34)]: their comparison, (c) vs (e) in Fig. 2, would greatly benefit from using equivalent combinations $\theta_{1,2,3}$ defined on the corresponding quasidegenerate subspace (cf. $23E\oplus 15A_1$ in Table III of Ref. 34).

[31] C. Jaffé and W. P. Reinhardt, J. Chem. Phys. **77**, 5191 (1982). The long-term regular behavior of irregular trajectories close in energy to $\Pi_{4,5,6}$ is correlated with the latter as shown in Fig. 5 of this reference.
[32] The Poincaré indices of stationary points $\Pi_{1,2,3}$, $\Pi_{4,5,6}$, and $\Pi_{7,8}$ on CP_2 are the same as in the two-mode analysis: $+1$, -1, and $+1$.
[33] As in the 2D case (Refs. 31 and 35) these degenerate trajectories are unstable with "strongly chaotic" regions near the turning points.
[34] G. Hose and H. S. Taylor, J. Chem. Phys. **76**, 5356 (1982); also R. T. Swimm and J. B. Delos, *ibid.* **71**, 1706 (1979), Table II. $A+E$ triads ($l=0$, ± 2 or ± 1, ± 3 etc) are well seen in these and other quantum calculations on the Hénon–Heiles system.
[35] K. Stefanski and H. S. Taylor, J. Chem. Phys. **31**, 2810 (1985).
[36] Relations (5) can be well illustrated by invariant homogeneous polynomials: $|A_1\rangle=(x^2+y^2)/2$, $|E_x\rangle=(x^2-y^2)/2$, and $|E_y\rangle=xy$. If one of the C_2 axes coincides with axis x then $\theta_1=x^2$, and two other functions are obtained from θ_1 by the C_3 rotations: $\theta_{2,3}=[-(1/2)x\pm(\sqrt{3}/2)y]^2$.
[37] M. J. Davis and E. J. Heller, J. Chem. Phys. **75**, 246 (1981). Cf. the $\psi_{1,2}$ combinations these authors discuss for a C_2 symmetric two-mode problem with our $\theta_{1,2,3}$.
[38] The polar coordinates, appropriate to the study of the isotropic 2D oscillator, are $r=(q_{2x}^2+q_{2y}^2)^{1/2}$, $\tan\varphi=q_{2x}/q_{2y}$. Detailed discussion can be found elsewhere (Ref. 30), e.g., C. Cohen-Tannoudji, B. Diu, and F. Laloë, *Quantum Mechanics* (Hermann, Paris, 1977), Vol. I, Chaps. H_V and D_{VI}.
[39] W. Meyer, P. Botschwina, and P. G. Burton, J. Chem. Phys. **84**, 891 (1986).
[40] J. Tennyson and J. R. Henderson, J. Chem. Phys. **91**, 3819 (1989); J. R. Henderson and J. Tennyson, Chem. Phys. Lett. **173**, 133 (1990).
[41] S. Carter and W. Meyer, J. Chem. Phys. **93**, 8902 (1990); R. M. Whitnell and J. C. Light, *ibid.* **90**, 1774 (1989).
[42] P. N. Day and D. G. Truhlar, J. Chem. Phys. **95**, 6615 (1991); Z. Bačić and J. Z. H. Zhang, Chem. Phys. Lett. **184**, 513 (1991).
[43] J. Tennyson and B. T. Sutcliffe, Mol. Phys. **51**, 887 (1984).
[44] J. R. Henderson, C. R. Le Sueur, and J. Tennyson, Comput. Phys. Commun. *75*, 379 (1993).
[45] Overlapping of polyads in energy should not be considered as an ultimate limit for the validity of the polyad approximation. In our case the highest-in-energy, or circular states of Nth polyad first become close with the lowest-in-energy, or localized bending states of the $(N+1)$th polyad, so that despite being close in energy such states do not significantly interact due to very different localization patterns (Ref. 11).
[46] Splitting between the l components of a polyad, such as ΔE in Table III can be (roughly) approximated as proportional to $l^2-(l-2)^2$. Therefore only a substantial deviation from the $l-1$ dependence might indicate the formation of clusters of low-l levels. On the other hand, splitting within the $l=3$ components is an obvious indication of clustering.
[47] We comment only on few regular features of the ν_1, ν_2 interaction essential to the discussion of the states we consider. A more extensive analysis and assignment of the vibrational states of H_3^+ and D_3^+ by C. R. Le Sueur, N. Fulton, and S. Miller has been performed, but is as yet unpublished.
[48] C. Jaffé and M. E. Kellman, J. Chem. Phys. **92**, 7196 (1990).